Biomass and Bioenergy 127 (2019) 105282

Contents lists available at ScienceDirect

Biomass and Bioenergy

journal homepage: www.elsevier.com/locate/biombioe

Research paper

Boosting carbon efficiency of the biomass to liquid process with hydrogen from power: The effect of H_2/CO ratio to the Fischer-Tropsch reactors on the production and power consumption

Mohammad Ostadi, Erling Rytter, Magne Hillestad*

Department of Chemical Engineering, Norwegian University of Science and Technology, NO-7491, Trondheim, Norway

ARTICLE INFO

Keywords:
Power and biomass to liquid
Fischer-Tropsch synthesis
Effect of H_2/CO feed ratio

ABSTRACT

Carbon efficiency of a biomass to liquid process can be increased from ca. 30 to more than 90% by adding hydrogen generated from renewable power. The main reason is that in order to increase the H_2/CO ratio after gasification to the value required for Fischer-Tropsch (FT) synthesis, the water gas shift reaction step can be avoided; instead a reversed water gas shift reactor is introduced to convert produced CO_2 to CO. Process simulations are done for a 46 t/h FT biofuel production unit. Previous results are confirmed, and it is shown how the process can be further improved. The effect of changing the H_2/CO ratio to the Fischer-Tropsch synthesis reactors is studied with the use of three different kinetic models. Keeping the CO conversion in the reactors constant at 55%, the volume of the reactors decreases with increasing H_2/CO ratio because the reaction rates increase with the partial pressure of hydrogen. Concurrently, the production of C_{5+} products and the consumption of hydrogen increases. However, the power required per extra produced liter fuel also increases pointing at optimum conditions at a H_2/CO feed ratio significantly lower than 2. The trends are the same for all three kinetic models, although one of the models is less sensitive to the hydrogen partial pressure. Finally, excess renewable energy can be transformed to FT syncrude with an efficiency of 0.8–0.88 on energy basis.

1. Introduction

In the biomass to liquid process (BtL), woody biomass is converted to liquid hydrocarbons via Fischer-Tropsch (FT) synthesis. Even though BtL can include other technologies, the FT route is considered here. In the Fischer-Tropsch synthesis, hydrogen and CO react on a solid catalyst to form a diverse range of hydrocarbons and water. The stoichiometric H_2/CO molar ratio is slightly higher than two. However, when biomass is gasified, the product gas, i.e. the synthesis gas, or syngas, is hydrogen deficient and has a low H_2/CO ratio (usually less than one). In order to increase the ratio to a level that is suitable for Fischer-Tropsch synthesis, the conventional strategy is to add steam to syngas and, by use of a water gas shift reactor (WGS), shift part of the CO with water to CO_2 and hydrogen and hence increase the H_2/CO ratio. This results in more than half of the biomass carbon ending up as CO_2 and not in the product. Without adding extra energy to the process, a large carbon loss is inevitable. The limitation is connected to the conservation of energy.

An alternative to shifting the syngas to increase the H_2/CO ratio, is to add external energy in the form of hydrogen to the process, often referred to as Power and Biomass to Liquids or PBtL. There are studies in the literature and a few patents where this is suggested. Agrawal et al. [1] proposed a hybrid hydrogen-carbon process for production of liquid hydrocarbon fuels where the biomass acts as the carbon and energy source and hydrogen as an energy carrier supplied from carbon-free energy source. Bernical et al. [2] suggested to keep the WGS reactor on part of the syngas to increase the H_2/CO ratio, in addition to using hydrogen from high temperature steam electrolysis to adjust the H_2/CO ratio to the required ratio for the FT synthesis. In another study, Peduzzi et al. [3] addressed the techno-economic evaluation and optimization of processes converting lignocellulosic biomass into liquid fuels including external H_2 addition. FT is among their considered processes. Hannula [4] investigated gasification of woody biomass to produce fuels like gasoline and methane with the addition of external hydrogen. Compared to reference plants, his calculations indicate that by adding external hydrogen, the fuel output can be increased by a factor of 2.6 and 3.1 for gasoline and methane, respectively. He calculated that a levelized cost of hydrogen below 2.2–2.8 €/kg will make the process competitive to the reference process. Seiler et al. [5] also reported a significant increase in BtL fuel production by means of external energy input. They calculated yields and energy inputs for

* Corresponding author.
E-mail addresses: mohammad.ostadi@ntnu.no (M. Ostadi), erling.rytter@ntnu.no (E. Rytter), magne.hillestad@ntnu.no (M. Hillestad).

https://doi.org/10.1016/j.biombioe.2019.105282
Received 24 October 2018; Received in revised form 17 June 2019; Accepted 20 June 2019

various process alternatives as well as cost estimation of those concepts. In another research, Dietrich et al. [6] presented three process concepts where hydrogen water electrolysis is applied in a reversed water gas shift (RWGS) reactor to shift CO_2 to CO in order to increase the carbon efficiency. They compared three different process concepts; (a) the conventional BtL without any addition of hydrogen, (b) using renewable power to produce hydrogen combined with BtL and (c) to convert CO_2 from combustion to produce CO and further to Fischer-Tropsch products.

Recently, Hillestad et al. [7] further developed and improved the BtL concept with addition of renewable hydrogen by using a detailed model of the process. Extra energy is added as hydrogen produced from renewable power. Hydrogen is produced through high temperature steam electrolysis in a solid oxide electrolysis cell (SOEC), with high temperature steam generated from the hot syngas. The oxygen produced from the SOEC is sufficient as oxidant in a biomass gasifier, thereby eliminating the need for a cryogenic air separation unit. Compared to alkaline water electrolysis, high temperature steam electrolysis requires less electrical power [8].

The present study investigates electricity input to a biomass-based FT process to determine the effect on renewable carbon utilization. In particular, the effect of the H_2/CO feed ratio in the syngas to the FT reactors is studied. The robustness of the Fischer-Tropsch reactor simulations is investigated based on three published kinetic expressions that are fitted to a common experimental dataset. This process concept reduces the CO_2 release from conventional biomass to liquid plants and has the potential for reducing the price of advanced biofuel for the aviation industry [7].

2. Process concept

A simplified block flow diagram of the PBtL process is shown in Fig. 1. While a detailed process description is given by Hillestad et al. [7], a short description is provided here. The biomass is pretreated by drying, torrefaction and grinding to reduce its particle size and moisture mass fraction. In the biomass pretreatment step, the biomass is dried, torrefied and grinded. Torrefaction has been proved to be one of two options when considering entrained flow (EF) gasification of wood [9]. Torrefaction improves grindability of the wood [10,11] and gives a particle size distribution which is suitable for EF gasification. The alternative, pyrolysis, has not been considered here. The torrefaction unit is integrated with the gasifier, with the consequence that there will be no loss of carbon as heat from the process is utilized. This means that volatiles from the torrefaction unit are added to the gasifier.

In the entrained flow gasifier, torrefied biomass is converted to syngas in the presence of oxygen. There is no need for cryogenic air separation as oxygen is produced in the SOEC. Sufficient oxygen is used for biomass gasification to obtain a temperature of about 1600 °C. The high temperature in the entrained flow gasifier causes melting of ash and thermal cracking of tars with high carbon conversion [12]. Low ash and tar content in the gas product leads to simpler downstream gas cleaning units. However, EF gasifier requires small particle sizes, typically below 1 mm in order to achieve high conversion rates [9].

The produced syngas is very reactive at high temperatures. By addition of hydrogen from the SOEC, the RWGS reaction is promoted and the H_2/CO ratio of the syngas is adjusted to the pre-set value. In this way, the amount of CO_2 in the syngas stream is minimized, thus improving carbon efficiency which is an indication of the amount of biomass carbon ending up in products. Note that the shift reactor is an integral part in the top of the gasifier. The still very hot syngas is quenched through the waste heat boiler (WHB) by evaporating water at ca. 11.7 MPa and 322 °C, and the generated steam is further superheated to 700 °C. The produced steam is partly used for pretreatment of the biomass while the main part is used as feed to the SOEC. For the latter purpose, the steam is further heated to 850 °C in a fired heater, fueled by the purge gas and combusted with air. The generated exhaust gas of the fired heater contains the first part of the residual CO_2 emission of the process. SOEC cannot withstand a pressure of 11.7 MPa, so the pressure is reduced to 4 MPa over a reduction valve prior to the fired heater. In our SOEC model, 80% of water is converted to H_2 and O_2. Oxygen migrates through the solid oxide membrane, producing a neat oxygen stream while hydrogen and unconverted water exit collectively. The produced hydrogen stream is cooled down to 50 °C to condense its water content (not shown). Part of the hydrogen is sent to the second and third FT reactors and to the upgrading unit, but the majority is reheated to 750 °C by heat exchange with the produced H_2 stream and used for the RWGS. The resulting water stream needs no further processing and is reheated and used in the SOEC.

Removal of H_2S is necessary to reach the feed gas specification required for FT synthesis; here assumed to be 10 μg/kg [13]. It is desired to have minimum H_2 and CO losses during the acid gas removal in order to retain the desired H_2/CO ratio for FT synthesis. Considering these requirements, acid gas removal based on physical solvents is used in this study [14]. Among the commercial physical solvents and technologies, Selexol has been selected since it does not require intensive solvent refrigeration or thermal regeneration. By using an absorption type process, some CO_2 is unavoidably extracted as well. In all cases it is assumed that 90% of the remaining CO_2 after RWGS is extracted in the acid gas removal unit. This amount of CO_2 constitutes the second source of residual CO_2 emission. Depending on the H_2/CO ratio used in FT reactors, the amount of CO_2 extracted can be as low as 10.5 t/h (for H_2/CO = 2.05) and 11.5 t/h (for H_2/CO = 1.6). The H_2S concentration achieved by the Selexol system is about 1 mg/kg. Chemical adsorption in a ZnO bed, not shown in Fig. 1, is used to further reduce the H_2S concentration to the FT requirements.

The Fischer-Tropsch section is divided into three different stages with separation of water and produced hydrocarbons after each stage. Syngas is preheated and converted in the FT reactors at a temperature of 210 °C. The selected slurry reactors are well back-mixed meaning that the exit gas composition is characteristic for the composition throughout the reactors. Further characteristics of the reactors are excellent heat removal and scalability. More heavy hydrocarbons are produced with low H_2/CO ratio, but on the other hand; having a low H_2/CO ratio decreases the production rate [15]. Therefore, there is a trade-off between maximizing the selectivity to heavy hydrocarbons and the production rate. With an under-stoichiometric H_2/CO ratio, hydrogen is the limiting reactant and needs to be added to each FT stage. Note that an over-stoichiometric H_2/CO ratio has not been considered due to very unfavorable selectivities and the need to separate surplus hydrogen between reactor stages. With the resulting high once through CO conversion in excess of 91% the tail-gas volume is minimized. It consists mainly of some unconverted syngas and lighter hydrocarbons which are then recycled to the gasifier, apart from the fraction that is used as fuel. Finally, Fischer-Tropsch products are upgraded through hydrotreating, hydrocracking and separation through distillation.

Some further details of the process are given in the process flow diagram in Fig. 2. Temperature and pressure levels of important streams are shown. In addition, mass flow and composition of streams with bold tag numbers are given in Table 1.

3. Process modeling and simulation

Simulations and modeling of the process flowsheets are performed with the use of Aspen HYSYS V9. Existing modules in HYSYS are not used to model the FT reactors, as existing modules are incapable of having detailed reaction stoichiometry. Therefore, MATLAB CAPE-OPEN unit operation[1] is used for modeling the FT reactors within Aspen HYSYS.

[1] www.amsterchem.com.

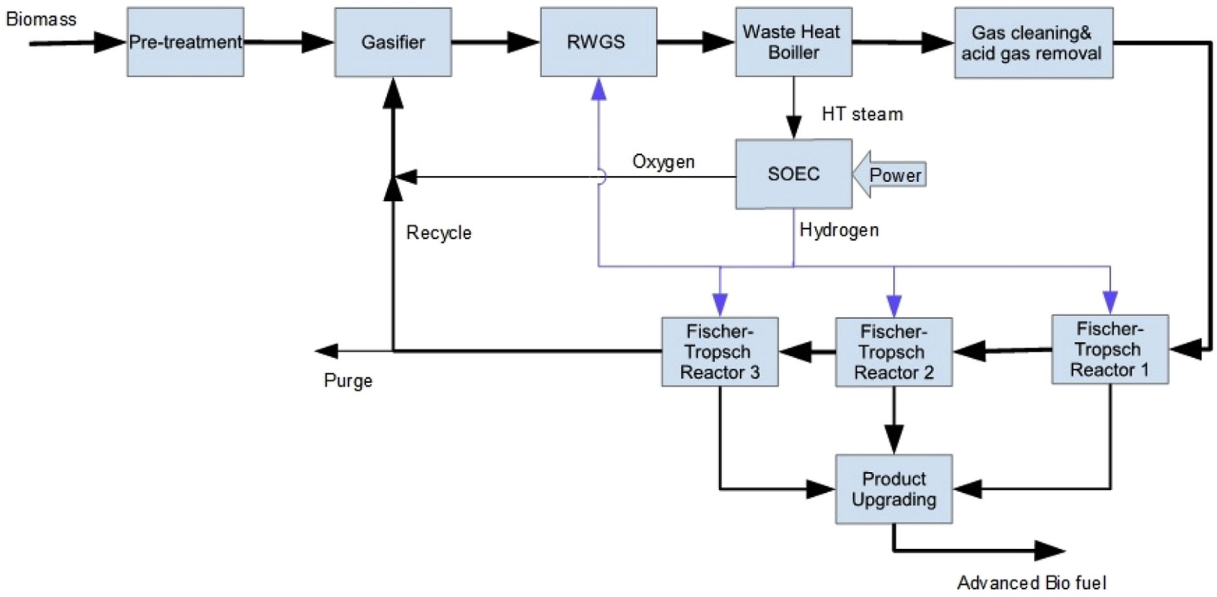

Fig. 1. Simplified block flow diagram of the PBtL process. Renewable hydrogen is shown in blue. (For interpretation of the references to colour in this figure legend, the reader is referred to the Web version of this article.)

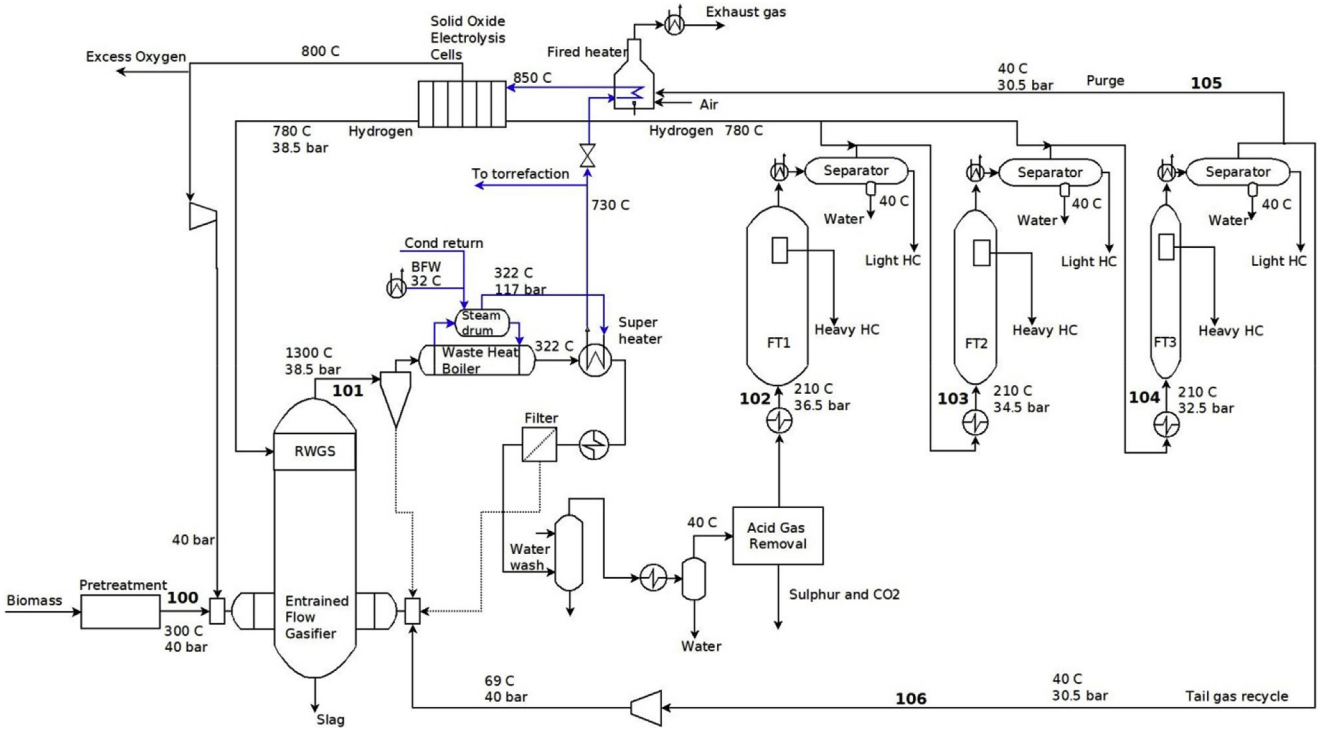

Fig. 2. Process flow diagram of the PBtL process. High temperature steam generation for SOEC is shown in blue. Details of streams with bold tag numbers are included in Table 1. (For interpretation of the references to colour in this figure legend, the reader is referred to the Web version of this article.)

3.1. Biomass

The biomass as a chemical component is introduced as a solid hypothetical component in HYSYS with elemental composition given in Table 2.

The heat of formation of biomass based on elemental composition is estimated by applying the method of Burnham [16], and the molar heat of formation is specified to be −0.5184 MJ/mol. Peduzzi et al. [17] provided correlations to estimate thermodynamic properties of biomass based on its elemental composition. Using their model, the heat of formation is within 5% of the above calculated value. An arbitrary molar mass of 100.11 g/mol is considered for the biomass. The wet biomass is assumed to have a moisture mass fraction of 40% which reduces to 5% after drying and torrefaction. The LHV of dry biomass is calculated to be 18.75 MJ/kg. All simulations are with the same thermal plant capacity of 435 MW based on the LHV of dry biomass which corresponds to 83.5 t/h of dry biomass.

3.2. Entrained flow gasifier with reverse shift

The gasifier is modeled using two model reactors in HYSYS: a conversion reactor followed by a Gibbs reactor. In the conversion

Table 1
Important stream information using kinetic Model 2 and H_2/CO molar ratio = 1.8

Stream	100	101	102	103	104	105	106
Temperature (°C)	300	1600	210	210	210	40	40
Pressure (bar)	40	38.5	36.5	34.5	32.5	30.5	30.5
Mass flow (t/h)	87.4	167.1	129.6	63.45	33.5	2.05	17.48
Molar flow (kmol/h)	1063	13,012	11,285	5226	2523	122	1048
Mole fractions							
Dry biomass	0.78	0	0	0	0	0	0
CO	0	0.307	0.353	0.341	0.317	0.305	0.305
H_2	0	0.552	0.636	0.614	0.571	0.438	0.438
H_2O	0.22	0.115	0.003	0.003	0.003	0.003	0.003
CH_4	0	0.001	0.001	0.018	0.053	0.129	0.129
C_2–C_4	0	0	0	0.007	0.021	0.051	0.051
CO_2	0	0.021	0.002	0.005	0.011	0.023	0.023
N_2	0	0.003	0.004	0.009	0.018	0.039	0.039

Table 2
The elemental composition of the biomass feedstock.

Element	Mass fraction (%) on dry basis and ash free material.
C	51.8
H	6.04
N	0.17
S	0.09
O	41.9

reactor, biomass is decomposed with a stoichiometry given by the biomass elemental composition into its constituent elements: C, H_2, N_2, O_2, and S. The Gibbs reactor takes the products from decomposition along with added steam and oxygen and calculates the equilibrium composition by minimizing the Gibbs free energy. In order to simulate an adiabatic gasifier, the heat released from the Gibbs reactor must be equal to the heat required by the decomposition reaction. The amount of oxygen determines the amount of heat released from the equilibrium reaction and hence the gasifier temperature. Since the gasifier is large, the relative heat loss is assumed negligible. The gasifier is operating at 1600 °C and 4 MPa, and at that high temperature it is a reasonable assumption to have chemical equilibrium and negligible amount of tar formation. The reverse water gas shift reactor is modeled as an equilibrium reactor by minimizing the Gibbs free energy. Injecting produced H_2 at 780 °C from the SOEC quenches the syngas temperature to about 1300 °C prior to RWGS section.

3.3. Fischer-Tropsch reactor

The Fischer-Tropsch reaction is a polymerization reaction in which carbon monoxide reacts with hydrogen to form n-paraffins, 1-olefins and oxygenates. By using cobalt catalyst, the major part of the products are paraffins and olefins;

$$n\mathrm{CO} + (2n+1)\mathrm{H_2} \rightarrow \mathrm{C}_n\mathrm{H}_{2n+2} + n\mathrm{H_2O} \quad \mathrm{n}= 1,2,\ ...,\ \infty$$

$$n\mathrm{CO} + 2n\mathrm{H_2} \rightarrow \mathrm{C}_n\mathrm{H}_{2n} + n\mathrm{H_2O} \quad \mathrm{n}= 2,3,\ ...,\ \infty$$

The above reactions do not account for the product distribution and need to be complemented with a chain growth or chain propagation model, α. The formation reactions of paraffins and olefins are lumped into two separate reactions, r_1 & r_2, where the stoichiometric coefficients are given by the Andersen-Schulz-Flory (ASF) distribution with two different growth factors, α_1 for paraffins and α_2 for olefins. The growth factor for olefins, α_2, is assumed to be ca. 70% of α_1 and, therefore, the olefin lump is lighter than the paraffin lump. The chain growth factors change with H_2/CO ratio, the temperature and the water partial pressure. Moreover, the selectivity to methane is higher than predicted by ASF and the selectivity towards ethylene is lower. In general, a separate methanation reaction, r_3, can be introduced to account for the observed distribution. Some variations are described below for each individual model. Further details and a consistent procedure for calculating stoichiometric coefficients have been presented previously [18].

$$\mathrm{CO} + U_1\mathrm{H_2} \xrightarrow{r1} \nu_{1,1}\mathrm{CH_4} + \nu_{1,2}\mathrm{C_2H_6} + ... + \nu_{1,10}\mathrm{C_{10}H_{22}} + \nu_{1,[11,\infty]}\mathrm{C}^P_{11+} + \mathrm{H_2O}$$

$$\mathrm{CO} + U_2\mathrm{H_2} \xrightarrow{r2} \nu_{2,1}\mathrm{CH_4} + \nu_{2,2}\mathrm{C_2H_4} + ... + \nu_{2,5}\mathrm{C_5H_{10}} + \nu_{2,[6,\infty]}\mathrm{C}^O_{6+} + \mathrm{H_2O}$$

$$\mathrm{CO} + 3\mathrm{H_2} \xrightarrow{r3} \mathrm{CH_4} + \mathrm{H_2O}$$

4. Kinetic models

In this study, the PBtL process is evaluated based on three different kinetic models and four different H_2/CO ratios at the inlet of the FT reactors. Model 1 was originally developed using the continuously stirred tank reactor (CSTR) experimental data by Todic et al. [19,20]. We fitted Model 2 and Model 3 to the same experimental data. Therefore, all three models have the same experimental basis, and are adapted for use in a back-mixed slurry reactor.

4.1. Model 1

This is a complex model based on experiments done in a stirred tank slurry reactor and a 0.48%Re–25%Co/Al_2O_3 catalyst on mass basis over a range of operating conditions (T = 478, 493, 503 K; P = 1.5, 2.5 MPa; H_2/CO = 1.4, 2.1; WHSV = 1.0–22.5 NL g^{-1} h^{-1}) [19,20]. The model describes individual reaction rates for each component with changing growth factor for each polymerization step. In general, the growth factors are functions of vacant sites, S,which again is a function of changing growth factors, making the model implicit. This makes the model complex and many iterations are required to reach the solution. Hillestad [18] simplified the original model and made it explicit, without much loss of accuracy. In addition, the simplified model provides an accurate description of the overall CO and H_2 consumption without calculating very many individual reaction rates. This simplified model is applied here.

4.2. Model 2

The second reaction rate expression applied here is based on the work by Outi et al. [21]. The model was originally developed for experiments on a 6.2% Co/Al_2O_3 catalyst on mass basis in a plug-flow fixed-bed reactor at atmospheric pressure and 523 K under differential conditions (conversion below 2%). The kinetic model requires to be complemented with a chain growth model, since it does not describe the product distribution, only CO consumption rate. A separate methanation reaction is added to account for the higher methane selectivity than predicted by the Anderson (ASF) distribution. The olefin production rate, r_2, is set to 8% of the paraffin production rate [19].

This rate model together with a separate methanation reaction and a chain growth model published by Ostadi et al. [15] are fitted to the CSTR experimental data of Todic et al. [22]. The fitted models are as follows:

$$r_1 = \frac{kP_{\mathrm{CO}}^{0.5}P_{\mathrm{H_2}}}{(1 + 2.569P_{\mathrm{CO}}^{0.5})^3}$$

$$r_2 = 0.08 * r_1$$

$$r_3 = 8.493(r_1 * (1-\alpha)^2) * \exp\left(-3225.277\left(\frac{1}{T} - \frac{1}{483}\right)\right)$$

$$k(T) = 1.012\exp\left(-10355.7\left(\frac{1}{T} - \frac{1}{483}\right)\right)$$

$$\alpha_1 = \frac{1}{1 + k_2(T)\frac{P_{H_2}^{0.18}}{P_{CO}^{0.2}P_{H_2O}^{0.19}}}$$

$$k_2(T) = 0.059\exp\left(-2347.334\left(\frac{1}{T} - \frac{1}{483}\right)\right)$$

$$\alpha_2 = \alpha_1 e^{-0.27}$$

4.3. Model 3

Finally, the third kinetic model tested in the PBtL process model, is the widely used Yates and Satterfield rate equation [23]. The equation was originally developed for experiments with 21.4%Co/MgO/SiO_2 catalyst on mass basis in a CSTR at 220-240 °C, 5–15 bar, H_2/CO ratios of 1.5–3.5 and CO conversions of 11–73%. The model is of the Langmuir-Hinshelwood (LH) type equation. This rate model together with the above mentioned separate methanation reaction and chain growth model [15], are fitted to the CSTR experimental data of Todic et al. [22]. Again, the olefin production rate is set to 8% of the paraffin production rate. The resulting expressions are:

$$r_1 = \frac{kP_{CO}P_{H_2}}{(1 + 7.5P_{CO})^2}$$

$$r_2 = 0.08 * r_1$$

$$r_3 = 9.165(r_1 * (1 - \alpha)^2) * \exp\left(-272.96\left(\frac{1}{T} - \frac{1}{483}\right)\right)$$

$$k(T) = 1.378\exp\left(-10650.9\left(\frac{1}{T} - \frac{1}{483}\right)\right)$$

$$\alpha_1 = \frac{1}{1 + k_2(T)\frac{P_{H_2}^{0.18}}{P_{CO}^{0.2}P_{H_2O}^{0.19}}}$$

$$k_2(T) = 0.0578\exp\left(-3286.0\left(\frac{1}{T} - \frac{1}{483}\right)\right)$$

$$\alpha_2 = \alpha_1 e^{-0.27}$$

5. Simulation results and discussion

To compare the kinetic models, it is imperative to either keep reactor volumes or CO conversions constant. Here, CO conversion in each FT stage is kept constant at 55%, resulting in once-through conversion of ca 91%. The amount of hydrogen addition to RWGS is adjusted such that the H_2/CO ratio out of RWGS is the same as the desired H_2/CO ratio to the first FT stage; therefore, there is no need for hydrogen addition to the first FT stage. It has previously been shown that this mode of operation increases carbon efficiency [7]. In all cases the amount of purge is adjusted to have enough heat in the fired heater to heat up steam to a temperature of 850 °C before the SOEC. Furthermore, 90% of CO_2 in the reverse shifted syngas is extracted in the acid gas removal unit which is equal to 7–8% of the carbon in the biomass feed. Summary of the results for the three kinetic models are given in Tables 3–5. The density of syncrude (C_{5+}) is assumed to be 800 kg/m^3.

5.1. Syncrude production and carbon efficiency

In the present context we define syncrude as the produced hydrocarbon fraction with carbon numbers 5 and above; i.e. the C_{5+} selectivity. Fig. 3a illustrates syncrude production and needed reactor volumes for different H_2/CO feed ratios. With all models, increasing the H_2/CO ratios results in smaller volumes to reach a CO conversion of 55% per stage. This is simply because the reaction rate is directly related to partial pressure of hydrogen; therefore, the reaction rate is enhanced with increasing partial pressure of hydrogen. The effect of high H_2/CO ratio on volume is significant for Models 2 & 3 where increased H_2/CO ratio from 1.6 to 2.05 results in volume reduction of ca. 50%. On the other hand, the reactor volumes are remarkably constant for Model 1 with only a 15% reduction. These differences show that the kinetic model can have direct bearing on optimizing the process

Table 3
PBtL process with kinetic Model 1 in FT reactors.

M1: Todic et al. [19,20]				
H_2/CO to FT reactors	1.6	1.8	1.9	2.05
Total FT volume (m^3)	930	796	771	793
Total FT syncrude production (t/h)	45.8	46.1	46.2	46.3
Total FT syncrude production (m^3/h)	57.235	57.621	57.732	57.910
Average chain growth factor	0.973	0.965	0.962	0.957
CO conversion (%)	90.9	91.4	90.8	90.8
H_2 addition to FT (t/h)	2.6	1.5	1.0	0.1
H_2 addition to RWGS (t/h)	8.4	9.9	10.7	11.8
Total H_2 added (t/h)	11.0	11.4	11.6	11.9
Carbon efficiency (%)	90.4	91.0	91.2	91.4
Steam to SOEC (t/h)	122.9	126.9	129.2	132.3
Required power in SOEC (MW)	373	385	392	401
CO_2 released (t/h)	15.115	14.227	13.969	13.568
CO_2 released (kg/L FT product)	0.26	0.25	0.24	0.23
Required electric power (kWh/L) for extra production	10.62	10.87	11.03	11.25
Recycle flow to the gasifier (t/h)	12.6	13.6	15.4	16.8

Table 4
PBtL process with kinetic Model 2 in FT reactors.

M2: Outi et al. [21]				
H_2/CO to FT reactors	1.6	1.8	1.9	2.05
Total FT volume (m^3)	1180	832	756	645
Total FT syncrude production (t/h)	46.0	46.1	46.3	46.4
Total FT syncrude production (m^3/h)	57.548	57.673	57.830	57.985
Average chain growth factor	0.945	0.939	0.937	0.934
CO conversion (%)	90.9	91.0	91.0	90.9
H_2 addition to FT (t/h)	3.0	1.9	1.2	0.3
H_2 addition to RWGS (t/h)	8.6	10.1	10.8	12.0
Total H_2 added (t/h)	11.6	11.9	12.1	12.3
Carbon efficiency (%)	90.8	90.9	91.1	91.3
Steam to SOEC (t/h)	128.8	132.5	134.3	137.0
Required power in SOEC (MW)	391	402	407	415
CO_2 released (t/h)	14.668	14.562	14.233	13.833
CO_2 released (kg/L FT product)	0.25	0.25	0.25	0.24
Required electric power (kWh/L) for extra production	11.06	11.35	11.46	11.65
Recycle flow to the gasifier (t/h)	16.1	17.3	18.2	19.5

Table 5
PBtL process with kinetic Model 3 in FT reactors.

M3: Yates and Satterfield [23]				
H_2/CO to FT reactors	1.6	1.8	1.9	2.05
Total FT volume (m^3)	1391	988	866	727
Total FT syncrude production (t/h)	45.9	46.2	46.2	46.3
Total FT syncrude production (m^3/h)	57.330	57.704	57.801	57.923
Average chain growth factor	0.946	0.940	0.938	0.934
CO conversion (%)	91.0	90.9	91.1	90.6
H_2 addition to FT (t/h)	3.0	1.8	1.2	0.3
H_2 addition to RWGS (t/h)	8.5	10.1	10.8	12.0
Total H_2 added (t/h)	11.5	11.9	12.1	12.3
Carbon efficiency (%)	90.4	90.9	91.1	91.3
Steam to SOEC (t/h)	128.4	132.5	134.1	137.1
Required power in SOEC (MW)	389	402	407	416
CO_2 released (t/h)	15.276	14.558	14.206	13.875
CO_2 released (kg/L FT product)	0.27	0.25	0.25	0.24
Required electric power (kWh/L) for extra production	11.09	11.34	11.45	11.68
Recycle flow to the gasifier (t/h)	15.7	17.8	18.0	20.0

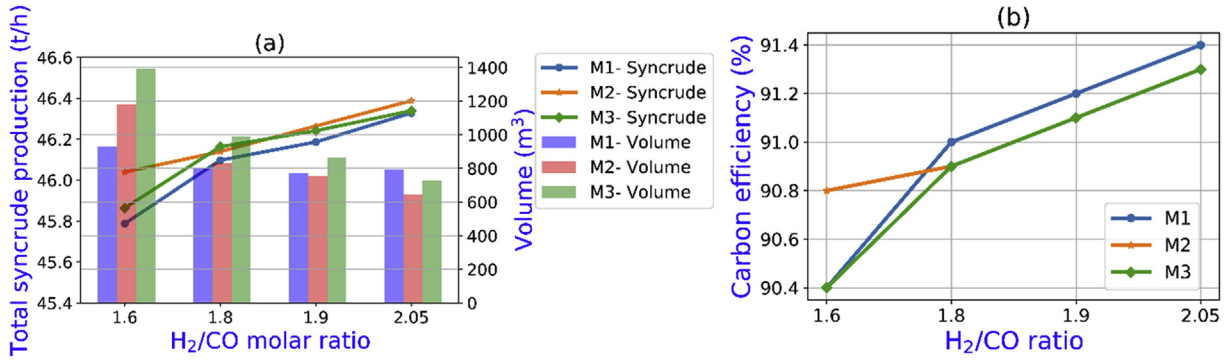

Fig. 3. a) Total syncrude production and required FT reactor volumes (bars) at constant CO conversion of 55% per stage for different H_2/CO feed ratios and kinetic models. b) Corresponding carbon efficiencies of the PBtL process. M1: Model 1; M2: Model 2; M3: Model 3.

conditions and configuration. There are also differences in total syncrude production between models and gas compositions, but the variations are relatively small ranging from 45.8 to 46.4 t/h. Still, the production increases systematically as the feed becomes richer in hydrogen. This is partly due to more conversion of CO_2 in the RWGS reactor. Consequently, less CO_2 is extracted in acid gas removal unit. Another reason for the increased production is due to a purge gas stream relatively rich in hydrogen, meaning that less methane is lost from the synthesis loop as fuel in the fired heater. Seemingly then, both from reactor volume and production point of view, there is an advantage to approach the stoichiometric consumption ratio in the feed gas. However, as is shown later, there is a trade-off with the power needed for hydrogen production.

Carbon efficiency is defined here as the percentage of biomass carbon that ends up in FT products containing at least five carbon atoms. Carbon efficiencies for the three different kinetic models are shown in Fig. 3b. Testing all kinetic models and all H_2/CO ratios, adding renewable hydrogen results in high carbon efficiencies; above 90% and typically threefold of a conventional BtL process. Concurrent responses of syncrude production and carbon efficiency can be inferred by comparing Fig. 3a and b. Nevertheless, Model 1 shifts the carbon efficiency to higher values than expected from the productivity chart. This special feature of Model 1 is again linked to low carbon loss in the fired heater as the model predicts higher chain growth factors and reduced methane formation; see the discussion below on tail-gas composition.

Details of the carbon flow are shown in Fig. 4a and b confirming the statements above concerning the effect of H_2/CO ratio on carbon efficiency; exemplified by Model 1 simulations. The carbon flow diagrams are practically indistinguishable from one kinetic model to another.

5.2. Hydrogen and power requirements

Increasing the H_2/CO ratio has positive effect on volume reduction and syncrude production, but on the other hand, there is need for more hydrogen to be added and, consequently, the need for more power to the SOEC. For each H_2/CO feed ratio and kinetic model, with the assumption of constant CO conversion in each FT reactor, there are forced responses in gas compositions. Most significantly, an increase in syncrude production requires more hydrogen. Hydrogen flow for the entire process is shown in Fig. 5a and b; again exemplified by Model 1 and H_2/CO ratios of 1.6 and 2.05, respectively. It reveals where the added hydrogen in the biomass and water ends up in the PBtL process streams and finally in the products. By increasing the H_2/CO ratio in the FT reactor feed, more hydrogen is needed for the RWGS (270 → 352) and less is needed between the FT stages (33 and 15→ < 5). In the latter case, more hydrogen is present in the recycle stream to the gasifier (39 vs. 18) and in the purge/fuel stream (5 vs. 3). With higher H_2/CO in the FT feed, more hydrogen is taken out in the form of water after the RWGS reactor.

In agreement with our previous study [7], there is a near linear relationship between added hydrogen and produced syncrude for a given kinetic model; see Fig. 6a. This relationship follows from the mass balance requirements; more product also means more hydrogen. The systematically less hydrogen needed for Model 1 is an inherent consequence of the model, favoring heavier products, although the same dataset was applied for all.

As shown in Fig. 6b, with all models, increasing the H_2/CO ratio from 1.6 to 2.05 requires ca. 0.8 t/h extra hydrogen to be added which is equivalent to 25 MW extra power. Therefore, there is a trade-off between hydrogen added and volume of reactors. This trade -off is highlighted in Fig. 7. To decide which H_2/CO ratio is beneficial, an important parameter is the required electric power for extra production of fuel compared to the case with no hydrogen addition; the conventional BtL process [7]. A significant finding is that low H_2/CO ratio is preferred irrespective of kinetic model as the electricity requirement per extra liter produced is lower. Model 1 requires the lowest power requirement among all models. We have not attempted to reduce the H_2/CO ratio below 1.6 as the reactor volumes show an exponential increase, cf. Fig. 3. A feed ratio of 1.6 means an actual H_2/CO ratio of 1.0 in a slurry reactor operating at 55% conversion; and 0.55 in the reactor for a feed ratio as low as 1.4. The spread shown in Fig. 7 in power needed per extra liter from 10.6 to 11.6 kWhr is significant. Still, the electric power required is on par with the lower heating value for

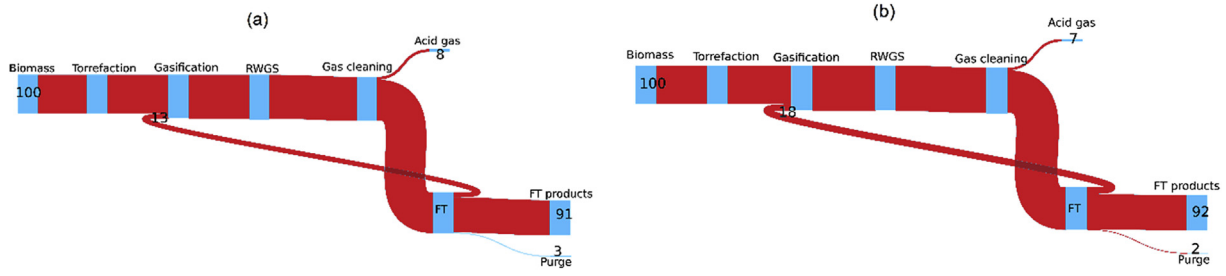

Fig. 4. Carbon flow using Model 1. a) H_2/CO ratio of 1.6. b) H_2/CO ratio of 2.05.

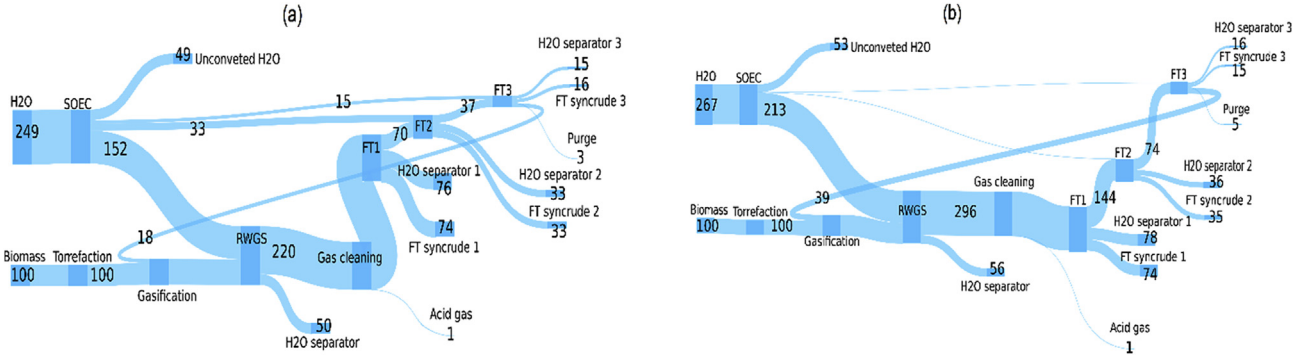

Fig. 5. Hydrogen flow using kinetic Model 1. a) H_2/CO ratio of 1.6. b) H_2/CO ratio of 2.05. Basis is 100 hydrogen present in the biomass.

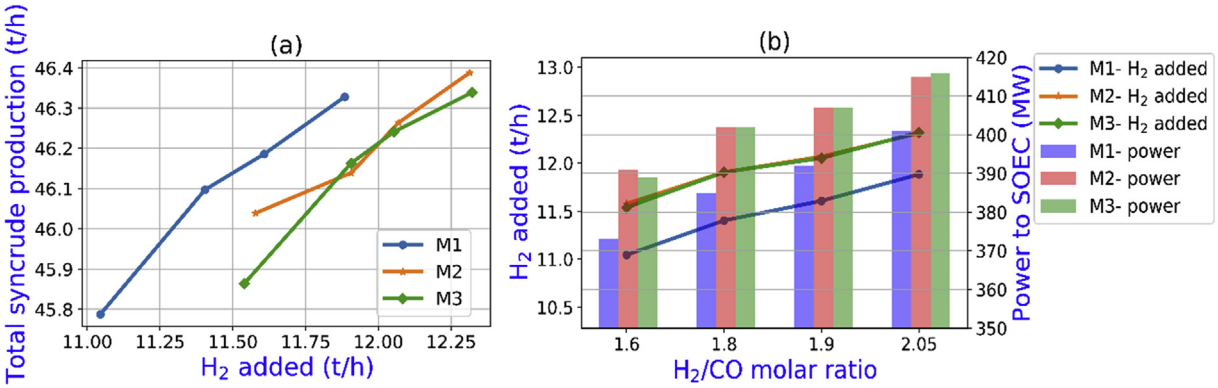

Fig. 6. Required renewable hydrogen addition for different H_2/CO feed ratios and kinetic models. a) Relationship to total FT production. b) Power requirement in SOEC (bars) and amount of hydrogen added.

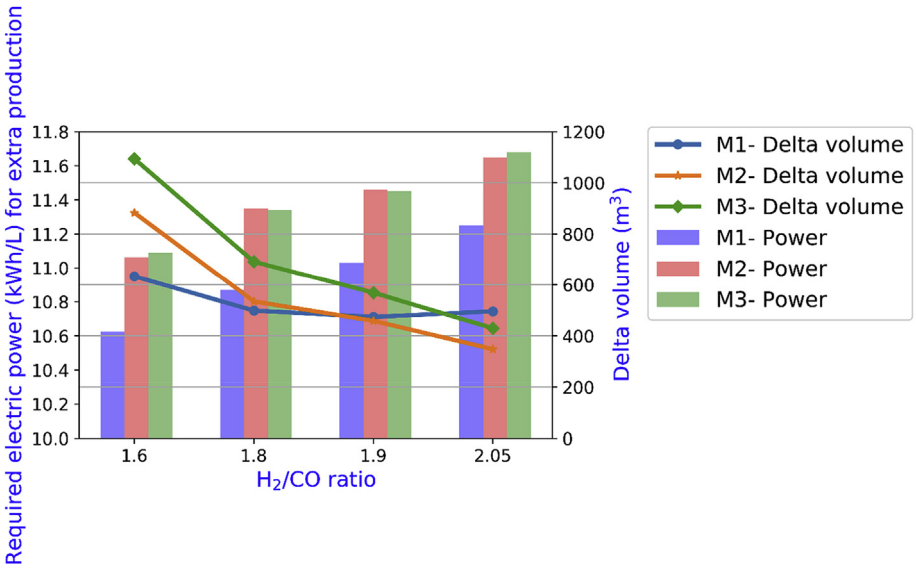

Fig. 7. Required power (bars) for water splitting for each extra liter of fuel with the PBtL concept compared to base case BtL for different H_2/CO feed ratios and three kinetic models. Difference in total volume requirement compared to the base case BtL is shown on the right vertical axis.

combusting this liter. Based on a LHV of 42 MJ/kg for a FT liquid and a density of 800 kg/m^3, the LHV is 33.6 MJ/L and 9.33 kWh/L. Thus, the energy in FT-product to input electrical energy is in the range of 0.80 - 0.88. This means that excess renewable energy can be transformed to FT syncrude with an efficiency of 0.8–0.88 on energy basis. These results are consistent with the results of Peduzzi et al. [3] who reported a ratio of about 0.84.

5.3. Tail-gas composition

As was mentioned above tail-gas composition plays an important role in optimizing carbon efficiency. Some of the tail-gas has to be purged anyway to avoid build-up of inert components. Therefore, a portion of the tail-gas is used in a fired heater to heat up the steam temperature before the SOEC. The composition in the tail gas affects the carbon efficiency. With a higher H_2/CO ratio to FT reactors, the tail gas contains more H_2. Therefore, less carbon is lost with the purge stream.

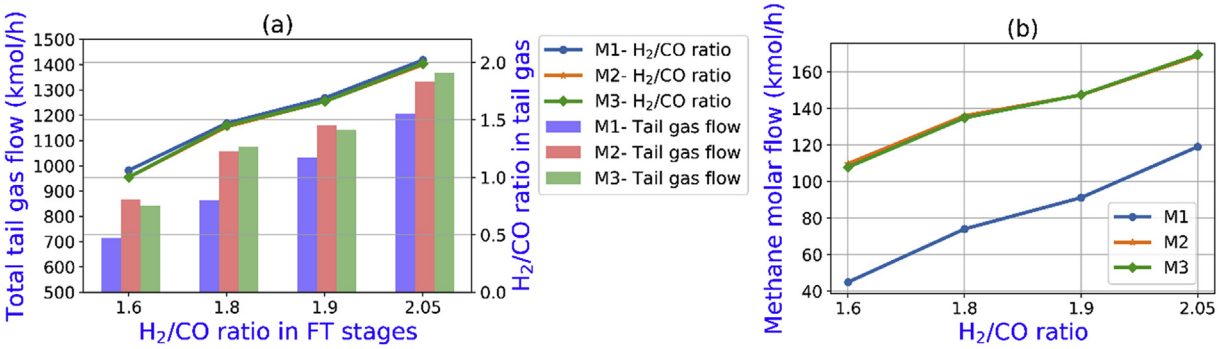

Fig. 8. Tail-gas flows and compositions for different H_2/CO feed ratios and three kinetic models. a) Dry tail-gas flows (bars) and H_2/CO ratio. b) Methane flow in tail-gas.

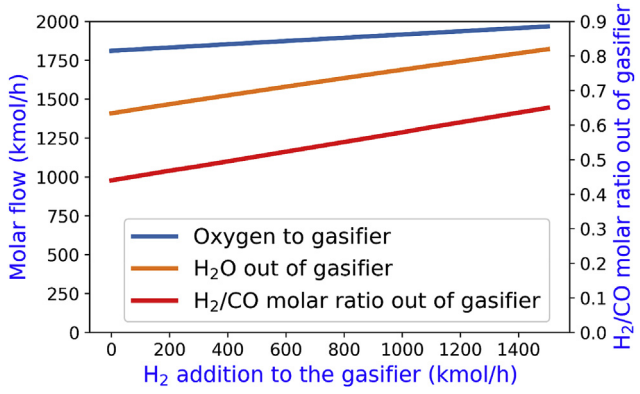

Fig. 9. Effect of H_2 in tail-gas on H_2O production and H_2/CO ratio out of gasifier.

Moreover, syngas contains less CO_2, which means less CO_2 is extracted in the acid gas removal. Less carbon in the tail-gas relative to hydrogen means a higher carbon efficiency. To be able to comprehend these interactions, the purge gas flows and compositions are investigated in Fig. 8a and b. Dry tail-gas consists of unconverted hydrogen and CO, some methane, and minor amounts of CO_2 and light hydrocarbons. First, note that the H_2/CO ratio in the purge gas, i.e. equal to the composition in the third FT reactor, varies considerably with the feed ratio. An under-stoichiometric feed requires high consumption of the available hydrogen relative to CO. As the consumption ratio varies marginally with conditions, all reactors have approximately the same internal H_2/CO ratio. Thus, increasing the H_2/CO ratio, results in a tail-gas composition significantly richer in hydrogen. On the other hand, the CO molar flow in the tail-gas stream remains almost constant, even by increasing the H_2/CO ratio, as it is mainly dictated by the CO conversion. As shown in Fig. 8a, the net result is higher total tail-gas flow containing more hydrogen as the syngas feed becomes richer in hydrogen. Consequently, less carbon is lost in the fired heater and the carbon efficiency and production increases; cf. Figs. 3 and 4.

Fig. 8b shows that there is an expected, concurrent increase in methane flow with H_2/CO ratio; more hydrogen means more methane. Model 1 predicts lower methane production than the other two models. As a corollary to the tail-gas composition, it is interesting to analyze the consequence for performance of the gasifier. Fig. 9 illustrates the effect of adding different amounts of hydrogen to the gasifier, simulating tail-gas with varying composition. Addition of hydrogen results in increased oxygen consumption to keep the temperature at the set point of 1600 °C and as a result producing more water. More importantly, there still is a significant increase in H_2/CO ratio. Seemingly contradictory, with more hydrogen present in the tail gas, more hydrogen is required for the RWGS reactor to meet the syngas specifications. This is illustrated in Fig. 5. This increase in hydrogen demand for reverse shift can be due to compensation for a high water vapor pressure in the gasifier. The overall result is that more syncrude is produced, but at the expense of electricity consumption in the SOEC as shown in Fig. 7. As a final point, in order to determine the optimal H_2/CO ratio of operation, three important factors are involved: the electricity price, with associated investment in water splitting, and the cost of reactors per unit volume as well as the syncrude price.

6. Conclusions

Three different kinetic models are implemented and tested within the PBtL process model. Their performances are compared using four different H_2/CO ratios at the inlet of three Fischer-Tropsch reactors in series. With all kinetic models and all H_2/CO ratios, adding hydrogen results in increased carbon efficiency, all above 90%. By increasing H_2/CO ratio to the FT reactors, more hydrocarbons are produced. Moreover, at constant CO conversion, the FT reactor volumes reduce with increasing H_2/CO ratio. With increasing H_2/CO ratio, the power consumption increases as more hydrogen is needed. On the other hand, decreasing the H_2/CO ratio in the syngas feed results in reduced requirement for power per extra liter syncrude. It is also shown that the selected kinetic model has direct consequence for how the reactor volumes respond to variations in H_2/CO ratio. This means that the choice of kinetic model will influence the selected operational conditions and process design. High selectivity to heavier hydrocarbons minimizes carbon loss through the purge gas and the acid gas removal unit. Finally, excess renewable energy can be transformed to FT syncrude with an efficiency of 0.8–0.88 on energy basis.

Acknowledgements

The research council of Norway (RENBTL project, project No. 267989) is greatly acknowledged for the financial aid of this project.

References

[1] R. Agrawal, N.R. Singh, F.H. Ribeiro, W.N. Delgass, Sustainable fuel for the transportation sector, Proc. Natl. Acad. Sci. U. S. A. 104 (12) (2007) 4828–4833.
[2] Q. Bernical, X. Joulia, I. Noirot-Le Borgne, P. Floquet, P. Baurens, G. Boissonnet, Sustainability assessment of an integrated high temperature steam electrolysis-enhanced biomass to liquid fuel process, Ind. Eng. Chem. Res. 52 (22) (2013) 7189–7195.
[3] E. Peduzzi, G. Boissonnet, G. Haarlemmer, F. Maréchal, Thermo-economic analysis and multi-objective optimisation of lignocellulosic biomass conversion to Fischer–Tropsch fuels, Sustain. Energy Fuel. 2 (5) (2018) 1069–1084.
[4] I. Hannula, Hydrogen enhancement potential of synthetic biofuels manufacture in the European context: a techno-economic assessment, Energy 104 (2016) 199–212.
[5] J.M. Seiler, C. Hohwiller, J. Imbach, J.-F. Luciani, Technical and economical evaluation of enhanced biomass to liquid fuel processes, Energy 35 (9) (2010) 3587–3592.
[6] R.U. Dietrich, F.G. Albrecht, S. Maier, D.H. König, S. Estelmann, S. Adelung, Z. Bealu, A. Seitz, Cost calculations for three different approaches of biofuel production using biomass, electricity and CO2, Biomass Bioenergy 111 (2018) 165–173.

[7] M. Hillestad, M. Ostadi, G.d. Alamo Serrano, E. Rytter, B. Austbø, J.G. Pharoah, O.S. Burheim, Improving carbon efficiency and profitability of the biomass to liquid process with hydrogen from renewable power, Fuel 234 (2018) 1431–1451.
[8] J.D. Holladay, J. Hu, D.L. King, Y. Wang, An overview of hydrogen production technologies, Catal. Today 139 (4) (2009) 244–260.
[9] J.J. Hernández, G. Aranda-Almansa, A. Bula, Gasification of biomass wastes in an entrained flow gasifier: effect of the particle size and the residence time, Fuel Process. Technol. 91 (6) (2010) 681–692.
[10] M. Phanphanich, S. Mani, Impact of torrefaction on the grindability and fuel characteristics of forest biomass, Bioresour. Technol. 102 (2) (2011) 1246–1253.
[11] B. Arias, C. Pevida, J. Fermoso, M.G. Plaza, F. Rubiera, J.J. Pis, Influence of torrefaction on the grindability and reactivity of woody biomass, Fuel Process. Technol. 89 (2) (2008) 169–175.
[12] K. Qin, P.A. Jensen, W. Lin, A.D. Jensen, Biomass gasification behavior in an entrained flow reactor: gas product distribution and soot formation, Energy & Fuels 26 (9) (2012) 5992–6002.
[13] E. Rytter, E. Ochoa-Fernández, A. Fahmi, Biomass-to-Liquids by the Fischer-Tropsch Process, Catalytic Process Development for Renewable Materials2013, pp. 265-308.
[14] K. Arnold, M. Stewart, CHAPTER 7 - acid gas treating-reviewed for the 1999 edition by K. S. Chiou of paragon engineering services, inc, in: K. Arnold, M. Stewart (Eds.), Surface Production Operations: Design of Gas-Handling Systems and Facilities, second ed., Gulf Professional Publishing, Woburn, 1999, pp. 151–194.
[15] M. Ostadi, E. Rytter, M. Hillestad, Evaluation of kinetic models for Fischer–Tropsch cobalt catalysts in a plug flow reactor, Chem. Eng. Res. Des. 114 (2016) 236–246.
[16] A.K. Burnham, Estimating the Heat of Formation of Foodstuffs and Biomass, (2010).
[17] E. Peduzzi, G. Boissonnet, F. Maréchal, Biomass modelling: estimating thermodynamic properties from the elemental composition, Fuel 181 (2016) 207–217.
[18] M. Hillestad, Modeling the Fischer–Tropsch Product Distribution and Model Implementation, Chemical Product and Process Modeling, 2015, p. 147.
[19] B. Todic, W. Ma, G. Jacobs, B.H. Davis, D.B. Bukur, CO-insertion mechanism based kinetic model of the Fischer–Tropsch synthesis reaction over Re-promoted Co catalyst, Catal. Today 228 (2014) 32–39.
[20] B. Todic, W. Ma, G. Jacobs, B.H. Davis, D.B. Bukur, Corrigendum to: CO-insertion mechanism based kinetic model of the Fischer–Tropsch synthesis reaction over Re-promoted Co catalyst, Catal. Today 242 (2015) 386.
[21] A. Outi, I. Rautavuoma, H.S. van der Baan, Kinetics and mechanism of the fischer tropsch hydrocarbon synthesis on a cobalt on alumina catalyst, Appl. Catal. 1 (5) (1981) 247–272.
[22] B. Todic, W. Ma, G. Jacobs, B.H. Davis, D.B. Bukur, Effect of process conditions on the product distribution of Fischer–Tropsch synthesis over a Re-promoted cobalt-alumina catalyst using a stirred tank slurry reactor, J. Catal. 311 (2014) 325–338.
[23] I.C. Yates, C.N. Satterfield, Intrinsic kinetics of the Fischer-Tropsch synthesis on a cobalt catalyst, Energy & Fuels 5 (1) (1991) 168–173.